Electronic Supplementary Information

In situ construction of $NiCo_2O_4$ nanosheets on nickel foam for efficient electrocatalytic oxidation of benzyl alcohol

Min Xu,[ab] Jing Geng,[ab] Hui Xu,[ab] Shengbo Zhang,*[ab] and Haimin Zhang,*[ab]

[a.] *Key Laboratory of Materials Physics, Centre for Environmental and Energy Nanomaterials, Anhui Key Laboratory of Nanomaterials and Nanotechnology, Institute of Solid State Physics, HFIPS, Chinese Academy of Sciences, Hefei 230031, China. E-mail: zhanghm@issp.ac.cn, shbzhang@issp.ac.cn.*

[b.] *University of Science and Technology of China, Hefei 230026, China.*

Contents

1. Experimental section

1.1 Chemicals and materials

Hydrochloric acid (HCl), acetone (C_3H_6O), ethanol (CH_3CH_2OH), methanol (CH_3OH) and methylbenzene (C_7H_8) were purchased from Sinopharm Chemical Reagent Co., Ltd. Urea (AR, 99%), $Co(NO_3)_2 \cdot 6H_2O$ (AR, 99%), $Ni(NO_3)_2 \cdot 6H_2O$ (AR, 98%), benzyl alcohol (AR, ≥99%), benzaldehyde (AR, ≥98%), benzoic acid (AR, ≥99.5%) and potassium hydroxide (KOH) were purchased from Aladdin Reagent Company. Nickel foam (NF) was purchased from Kunshan Longshengbao Electronic Material Co., Ltd. Deionized water (DW) made by laboratory.

1.2 Pre-treatment of Nickel foam (NF)

The commercial NF was cut into 3 × 3 × 0.1 cm^3 slices. Then, it was sonicated for 15 min in HCl (1.0 M) and acetone solution. This was followed by rinsing with ethanol and deionised water. Finally, the NF was placed in a vacuum drying oven and dried at 60°C for 6 hours for use.

1.3 Preparation of $NiCo_2O_4$/NF

In typical preparation, 2 mM $Ni(NO_3)_2 \cdot 6H_2O$, 4 mM $Co(NO_3)_2 \cdot 6H_2O$ and 24 mM urea were dissolved in 50 mL deionized water to form mixed solution by stirring for 30 min. Next, the NF and the mixed solution were transferred to an autoclave (80 ml) with a Teflon liner and kept at 90°C for 12 hours. After cooling to room temperature, the product was sonicated in deionised water and dried under vacuum at 60°C for 6 hours. Finally, the samples were annealed at 300°C for 2 hours in an air atmosphere to obtain seaweed-like $NiCo_2O_4$/NF samples.

1.4 Catalysts characterization

The crystalline structures of samples were identified by the X-ray diffraction analysis (XRD, Philips X'pert PRO) using Nifiltered monochromatic CuKa radiation (λKα1 = 1.5418 Å) at 40 kV and 40 mA. Scanning electron microscope (SEM) images of the sample were obtained using SU8020 (Hitachi, Japan) with an accelerating voltage of 10.0 kV. Transmission electron microscope (TEM) images of the sample were obtained using JEMARM 200F operating at an accelerating voltage of 200 kV. High-resolution transmission electron microscope (HRTEM), scanning TEM images (STEM) and elemental mapping images of samples were obtained on a JEOL-2010 transmission electron microscope. X-ray photoelectron spectroscopy (XPS) analysis was performed on an ESCALAB 250 X-ray photoelectron spectrometer (Thermo, America) equipped with Al Kα1, 2 monochromatized radiations at 1486.6 eV X-ray source. Raman spectra were obtained using a LabRAM HR800 confocal microscope In situ Raman spectroscopy were recorded on RAMANRXN. ICN (Kaiser, America) with a Leica DM2500M microscope at a 532 nm laser source (Invictu STM laser; 400 mW laser power). The acquisition time for each spectrum was 40 s with no signal accumulation.

1.5 Electrochemical measurements

All electrochemical measurements were performed on a CHI 760E electrochemical workstation (CH Instrumental Corporation, Shanghai, China) with a typical three electrode system, with $NiCo_2O_4$/NF (1 × 1 cm^2) as the working electrode. An active area of 1 cm^2 was assumed to define the current density (scaled current data). All

electrochemical measurements were performed with agitation. For the Selective electrocatalytic oxidation (ECO) of benzyl alcohol, a Hg/HgO (in 1 M KOH solution) electrode was used as the reference electrode and a Pt wire was used as the counter electrode. For the overall water-splitting (OWP), a Hg/HgO electrode was used as the reference electrode and a $NiCo_2O_4$/NF was used as the counter electrode. The electrolyte (pH=13.7) was 10 mL 1.0 M KOH solution with or without 50 mM benzyl alcohol. The potentials were converted to RHE scale using the following Nernst equation: The measured potentials versus the reversible hydrogen electrode (RHE) were converted based on the following equation (1):

$$E_{(RHE)} = E_{(Hg/HgO)} + 0.098 + 0.059 \times pH \quad (1)$$

The scan rate for cyclic voltammetry (CV) and linear scan voltammetry (LSV) was kept at 10 mV s^{-1} and 5 mV s^{-1}, respectively. The long-term stability and efficiency of the synthesized samples were confirmed by using constant current test with a reaction time of 7200 s and potential of 1.6 V for 15 cycles.

1.6 Product analysis

For the quantification of benzyl alcohol and oxidation products present in the reacted solution, a FuLi GC system (FuLi, GC9790II) equipped with a flame ionization detector (FID) was used. The chromatographic separation was performed on an HP-FFAP capillary column of 30 m × 0.320 mm i.d. and × 0.25 μm film thickness (Agilent Technologies, USA). Using toluene as the extractant, firstly acidify the reacted solution with 4 M HCl, let stand for half an hour and wait for the crystallization of benzoic acid, then add 3ml of toluene to it, take out the supernatant

after shaking, repeat the extraction for three times as an analysis sample. A sample volume of 1 μL is injected into the chromatograph using a syringe with a range of 10 μL depending on the concentration range of the analyte present in the sample. The conditions selected for the analysis of benzyl alcohol and oxidation products are listed in Table S2. The detector and injector temperatures were 270 and 240 °C, respectively. The oven temperature program was 80 °C (held for 0.1 min), increased at 15 °C/min to reach 240 °C (held for 1 min). The carrier gas used was nitrogen at 1.5 mL/min. The air and hydrogen flow rates were 300 and 30 mL/min, respectively. The data from GC runs were analyzed using the analytical tools provided with the instrument. The resulting peaks were identified by comparing retention times and quantified against the area of peaks. Each sample was prepared in triplicate and injected five times to determine the mean. The benzyl alcohol conversion (%) and the selectivity (%) of the oxidation products were calculated using equations (2) and (3):

$$Conversion\ of\ benzyl\ alcohol = \frac{moles\ of\ benzyl\ alcohol\ reacted}{initial\ moles\ of\ benzyl\ alcohol}$$

(2)

$$Selectivity\ of\ benzoic\ acid\ product = \frac{moles\ of\ benzoic\ acid\ product}{moles\ of\ oxidation\ products}$$

(3)

The yield of benzoic acid formation was calculated using the equation (4):

$$Yield\ of\ benzoic\ acid\ = Conversion \times Selectivity\ of\ benzoic\ acid$$

(4)

The faradaic efficiency of benzoic acid formation was calculated using the equation

(5):

$$Faraday\ efficiency = \frac{m \times n \times F}{I \times t} \quad (5)$$

Where m is the number of moles of the product, n is the number of electrons obtained from the reactant to the product, F is Faraday constant (96485 C mol^{-1}), I is the current, and t is the time.

The ethanol, glycol and their oxidation products were quantitatively analyzed by the ^1H NMR methods using Bruker Avance-400 MHZ. For the quantification of 4-methylbenzyl alcohol, 4-bromobenzyl alcohol, cinnamic alcohol, 1-butanol and their oxidation products present in the reacted solution, a FuLi GC system (FuLi, GC9790II) equipped with a flame ionization detector (FID) was used. The carrier gas used was nitrogen at 1.5 mL/min. The air and hydrogen flow rates were 300 and 30 mL/min, respectively. For 4-methylbenzyl alcohol, the detector and injector temperatures were 250 °C. The oven temperature program was 40 °C (held for 3.0 min), increased at 30 °C/min to reach 200 °C (held for 0.1 min), increased at 45 °C/min to reach 240 °C (held for 1 min). For 4-bromobenzyl alcohol, the detector and injector temperatures were 300 °C. The oven temperature program was 40 °C (held for 0.5 min), increased at 50 °C/min to reach 200 °C (held for 0.1 min), increased at 15 °C/min to reach 245 °C (held for 0.5 min), increased at 5 °C/min to reach 255 °C (held for 0.5 min). For cinnamic alcohol, the detector and injector temperatures were 300 °C. The oven temperature program was 40 °C (held for 0.1 min), increased at 30 °C/min to reach 230 °C (held for 0.1 min), increased at 5 °C/min to reach 250 °C (held for 1 min). For 1-butanol, the detector and injector temperatures were 250 °C. The oven temperature

program was 40 °C (held for 3.0 min), increased at 30 °C/min to reach 200 °C (held for 1 min).

The furfuryl alcohol, 5-hydroxymethylfurfural, p-nitrobenzyl alcohol and their oxidation products were quantitatively determined by a HPLC (Waters 1525) equipped with an ultraviolet−visible detector and a 4.6 mm × 150 mm Shim-pack GWS 5 μm C 18 column. A mixture of solvents A and B was used as the mobile phase for elution. For furfuryl alcohol and 5-hydroxymethylfurfural, solvents A and B were an aqueous solution containing 5 mM ammonium formate and HPLC grade methanol. The separation and quantification were accomplished using an isocratic elution of 70% A and 30% B at a flow rate of 0.5 mL min^{-1}. For p-nitrobenzyl alcohol, solvents A and B were an aqueous solution containing 0.02 M phosphoric acid and HPLC grade methanol. The separation and quantification were accomplished using an isocratic elution of 40% A and 60% B at a flow rate of 1.0 mL min^{-1}.

Supplementary Figures

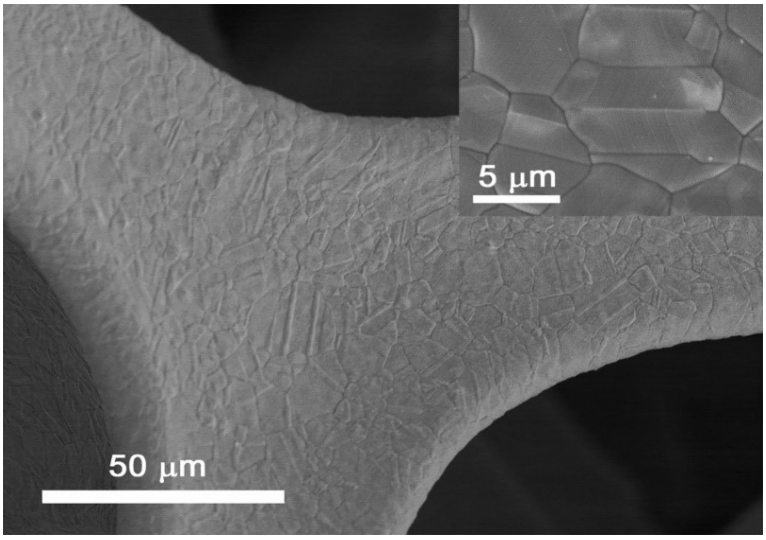

Fig.S1 SEM images of the treated NF.

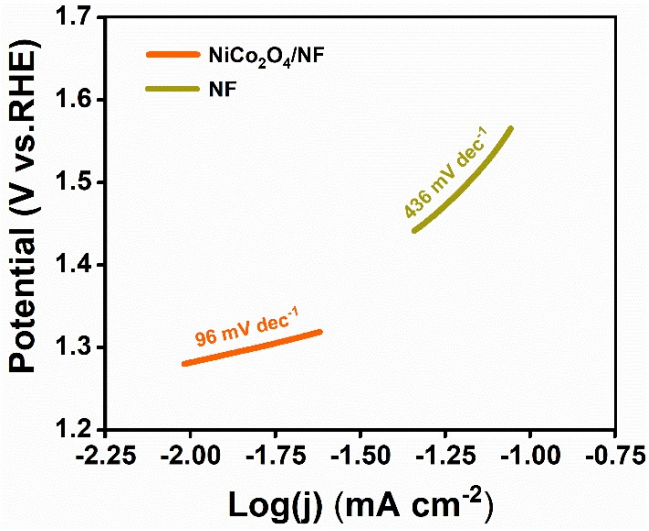

Fig.S2 Tafel plots of BA oxidation currents.

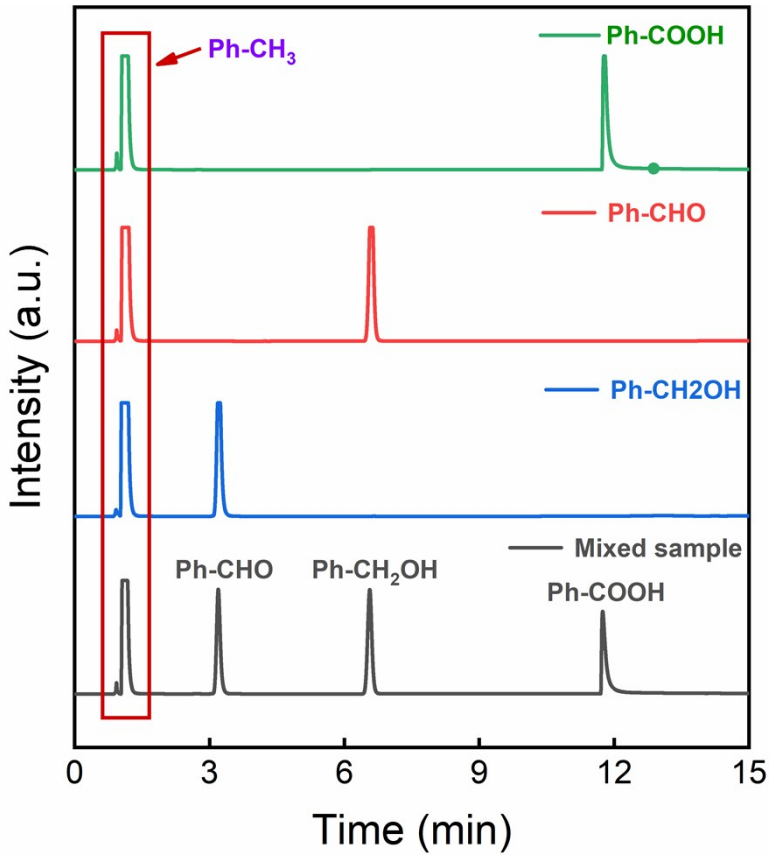

Fig.S3 GC chromatograms of benzoic acid, benzaldehyde, benzyl alcohol and the mixed sample.

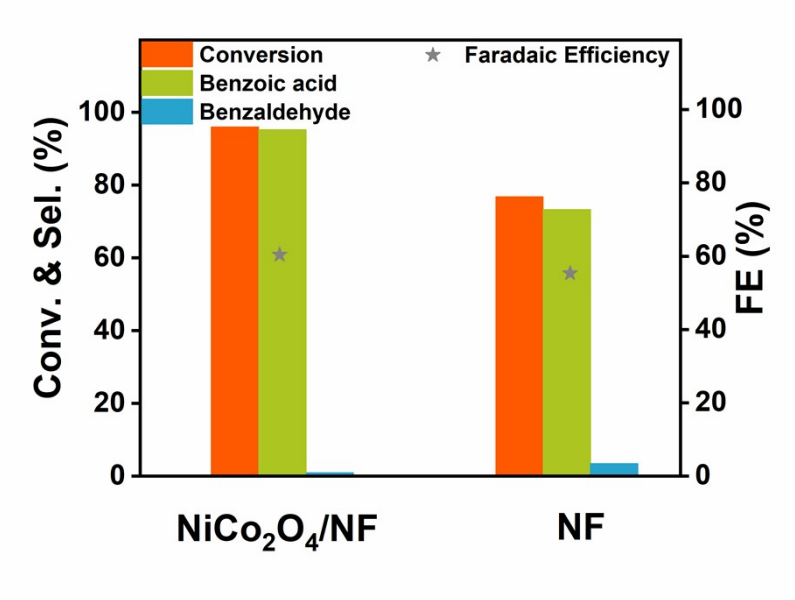

Fig.S4 Conversion of benzyl alcohol and selectivity to benzoic acid and benzaldehyde and faradaic efficiency in $NiCo_2O_4$/NF and NFunder potential of 1.6 V (*vs.*RHE) in 1.0 M KOH with 50 mM benzyl alcohol.

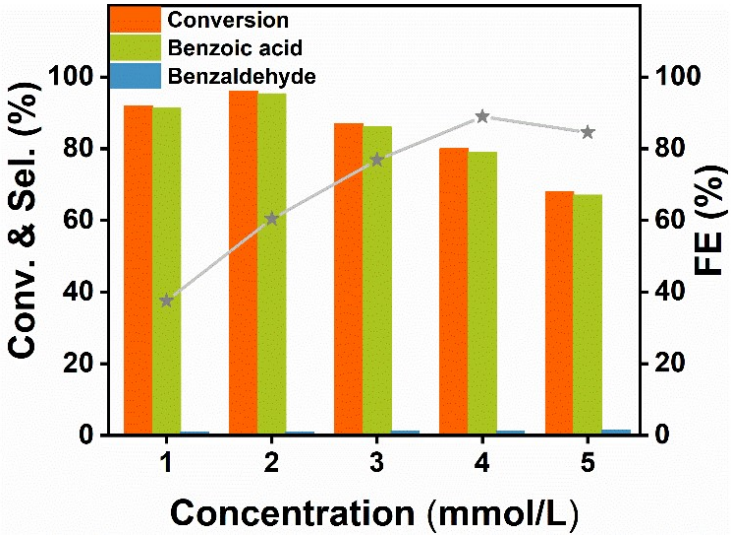

Fig.S5 Conversion of benzyl alcohol and selectivity to benzoic acid and benzaldehyde and faradaic efficiency under potential of 1.6 V (*vs.*RHE) in 1.0 M KOH with different benzyl alcohol concentrations.

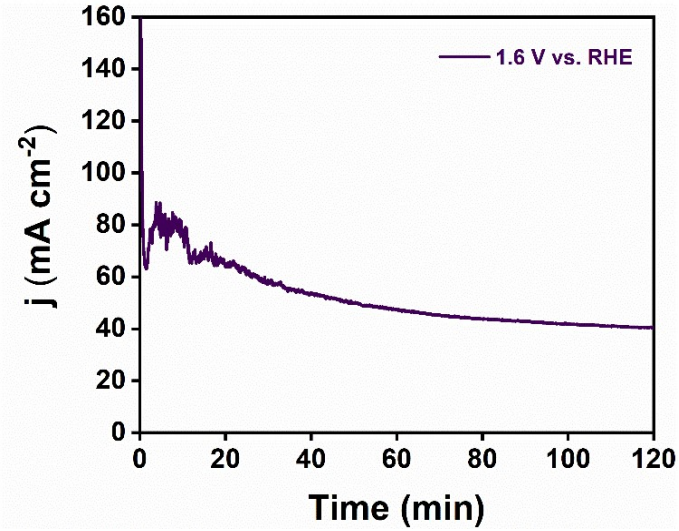

Fig.S6 Chronoamperometric curves of $NiCo_2O_4$/NF under potential of 1.6 V (vs. RHE) in 1.0 M KOH solution containing 50 mM benzyl alcohol.

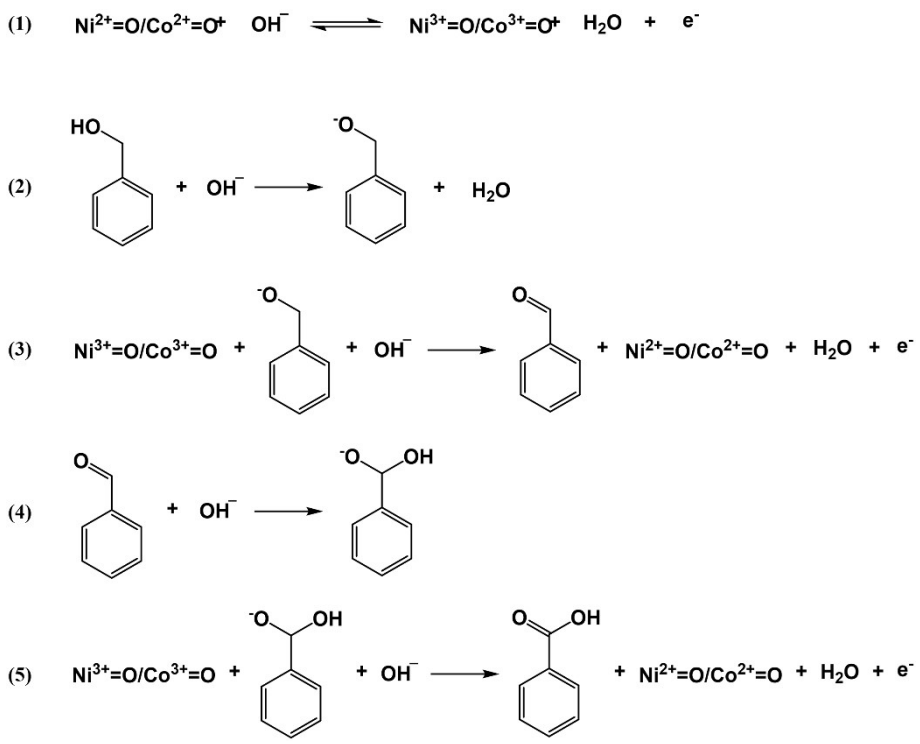

Fig. S7 Proposed mechanism of the benzyl alcohol oxidation on the $NiCo_2O_4$/NF membrane electrode.

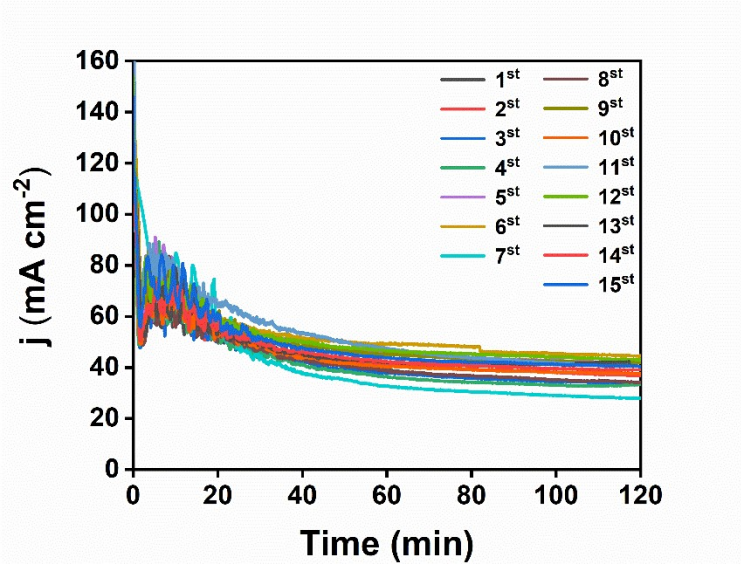

Fig.S8 Chronoamperometric curves of $NiCo_2O_4$/NF under potential of 1.6 V (*vs.* RHE) in 1.0 M KOH with 50 mM benzyl alcohol.

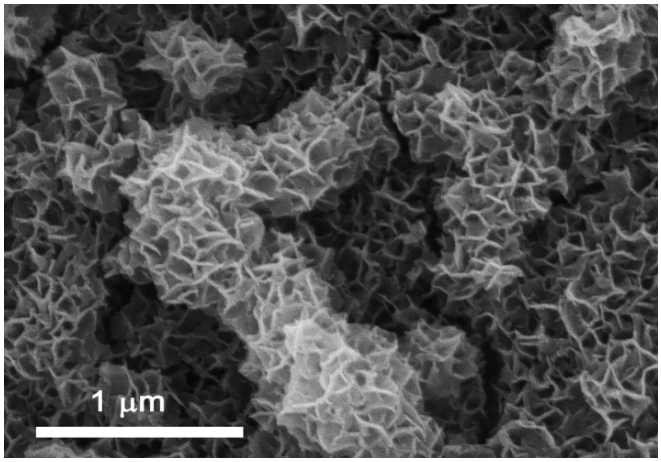

Fig.S9 SEM image of $NiCo_2O_4$/NF after 15 cycles of measurement.

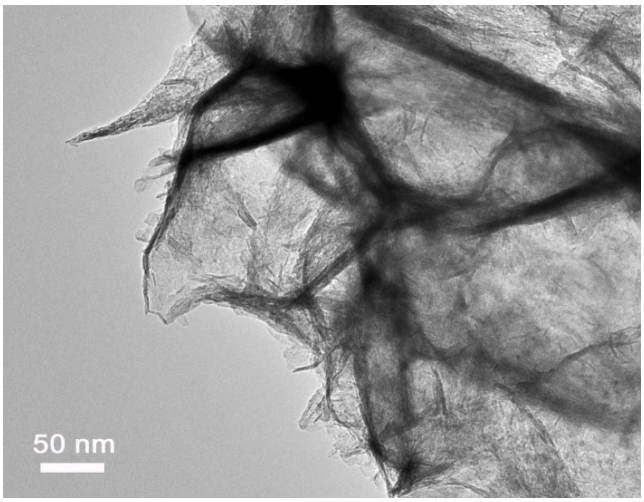

Fig.S10 TEM image of $NiCo_2O_4$/NF after 15 cycles of measurement.

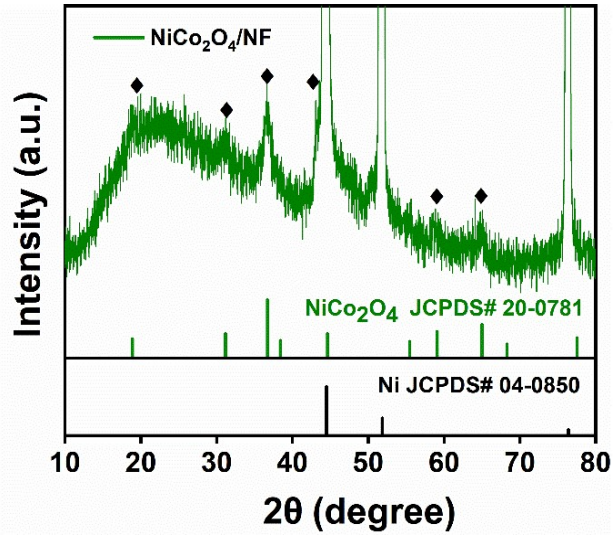

Fig.S11 XRD pattern of $NiCo_2O_4$/NF after 15 cycles of measurement.

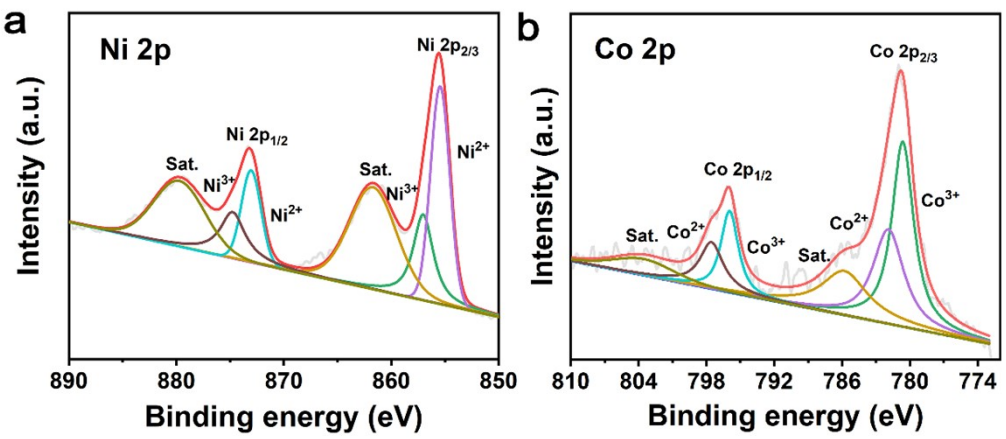

Fig.S12 High-resolution Ni 2p (a) and Co 2p (b) XPS spectra of $NiCo_2O_4$/NF after 15 cycles of measurement.

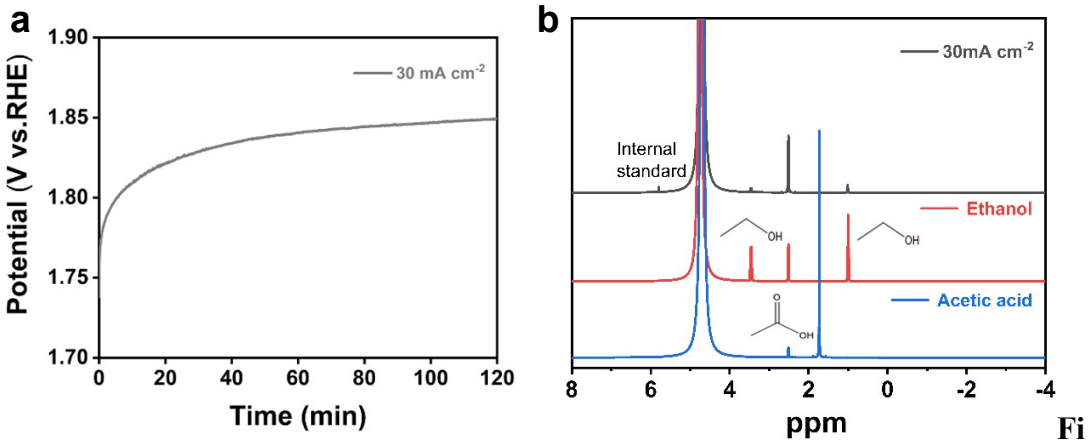

g.S13 (a) The chronopotentiometry curve of $NiCo_2O_4$/NF at the current density of 30 mA cm^{-2} in 1.0 M KOH solution containing 50 mM ethanol. (b) ^1H NMR spectra of ethanol, acetic acid and the electrolyte after 2 h anodic ethanol oxidation on a $NiCo_2O_4$/NF electrode using maleic acid as the internal standard.

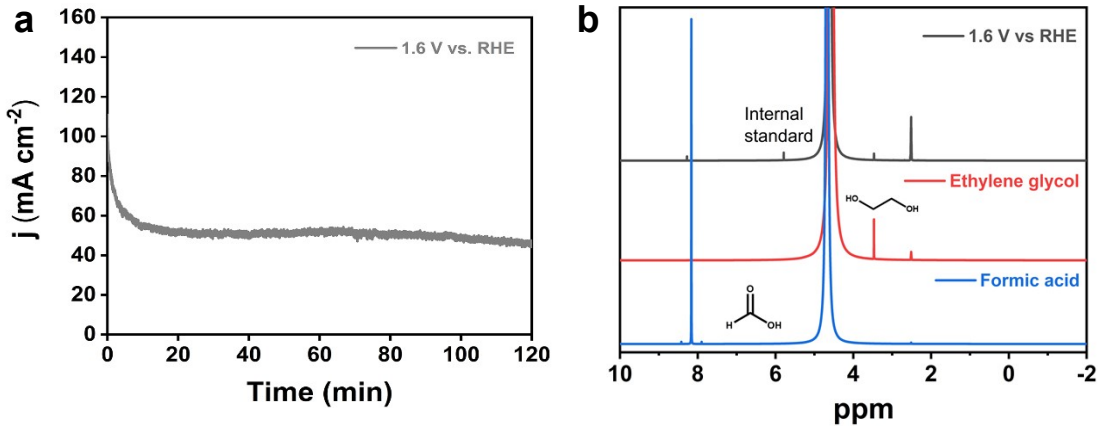

Fig.S14 (a) Time-dependent current density curve of $NiCo_2O_4$/NF under potential of 1.6 V (vs. RHE) in 1.0 M KOH solution containing 40 mM ethylene glycol. (b) ^1H NMR spectra of ethylene glycol, formic acid and the electrolyte after 2 h anodic ethylene glycol oxidation on a $NiCo_2O_4$/NF electrode using maleic acid as the internal standard.

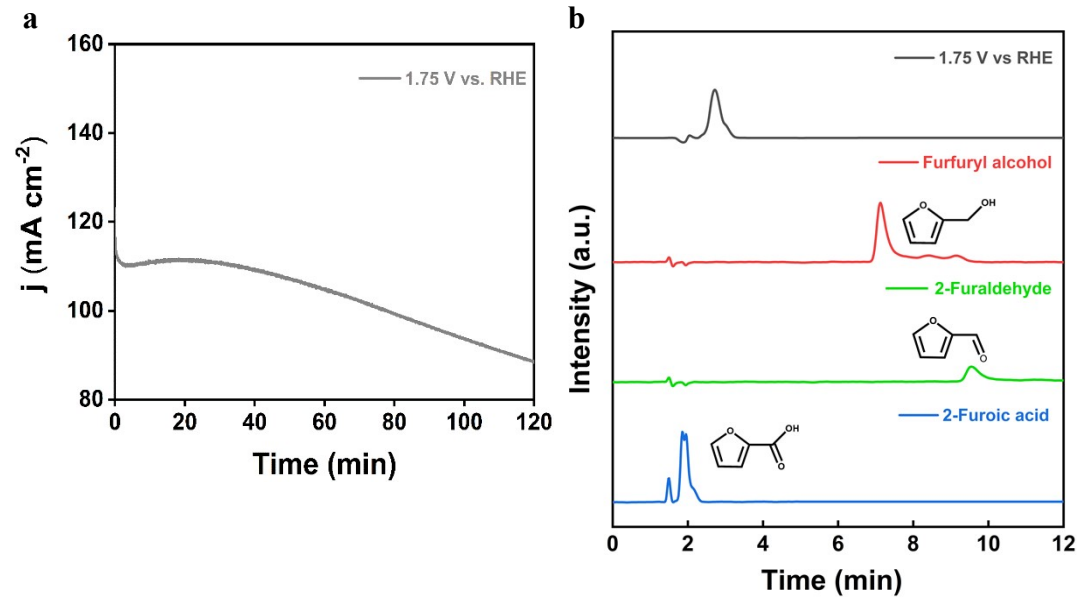

Fig.S15 (a) Time-dependent current density curve of $NiCo_2O_4$/NF under potential of 1.75 V (vs. RHE) in 1.0 M KOH solution containing 10 mM benzaldehyde. (b) HPLC chromatograms of furfuryl alcohol, 2-furaldehyde, 2-furancarbosylic acid and the electrolyte after 2 h anodic ethylene glycol oxidation.

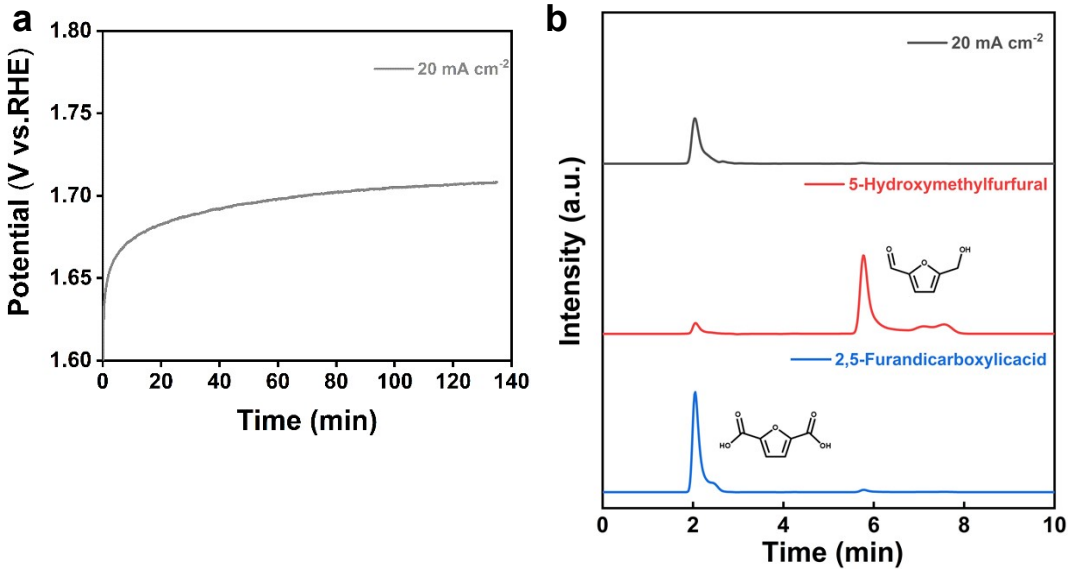

Fig.S16 (a) The chronopotentiometry curve of $NiCo_2O_4$/NF at the current density of 20 mA cm^{-2} in 1.0 M KOH solution containing 10 mM 5-hydroxymethylfurfural. (b) HPLC chromatograms of 5-hydroxymethylfurfural, 2,5-furandicarboxylic acid, and the electrolyte after 2.25 h anodic 5-hydroxymethylfurfural oxidation.

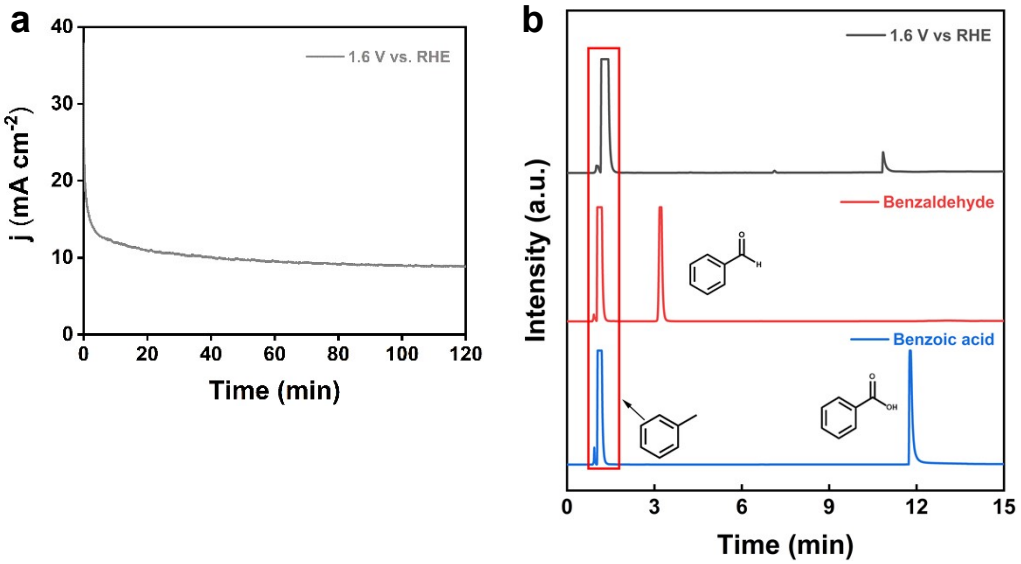

Fig.S17 (a) Time-dependent current density curve of $NiCo_2O_4$/NF under potential of 1.6 V (vs. RHE) in 1.0 M KOH solution containing 50 mM benzaldehyde. (b) GC chromatograms of benzaldehyde, benzoic acid and the electrolyte after 2 h anodic benzaldehyde oxidation.

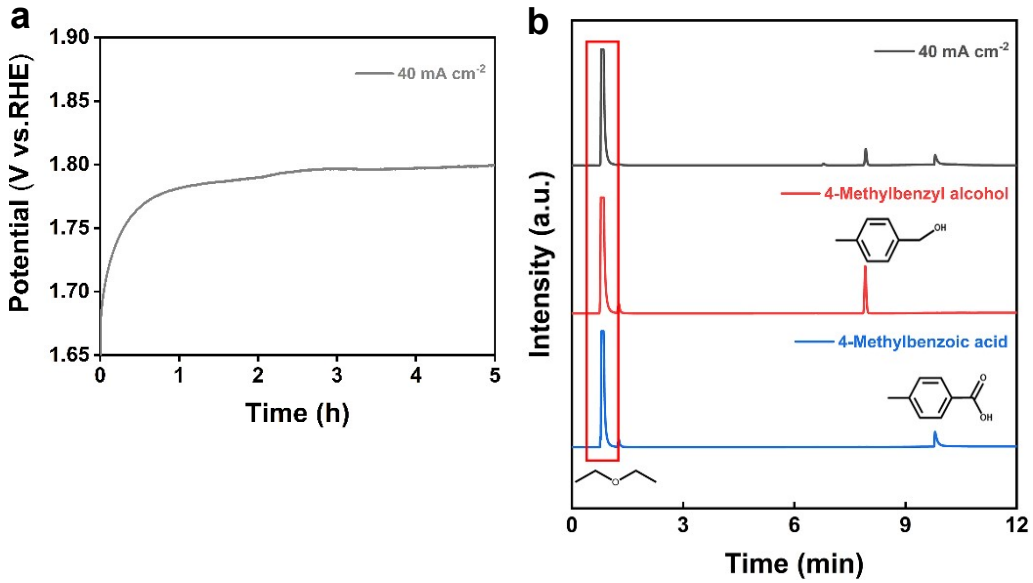

Fig.S18 (a) The chronopotentiometry curve of $NiCo_2O_4$/NF at the current density of 40 mA cm^{-2} in 1.0 M KOH solution containing 10 mM 4-methylbenzyl alcohol. (b) GC chromatograms of 4-methylbenzyl alcohol, 4-methylbenzoic acid and the electrolyte after 5 h anodic 4-methylbenzyl alcohol oxidation.

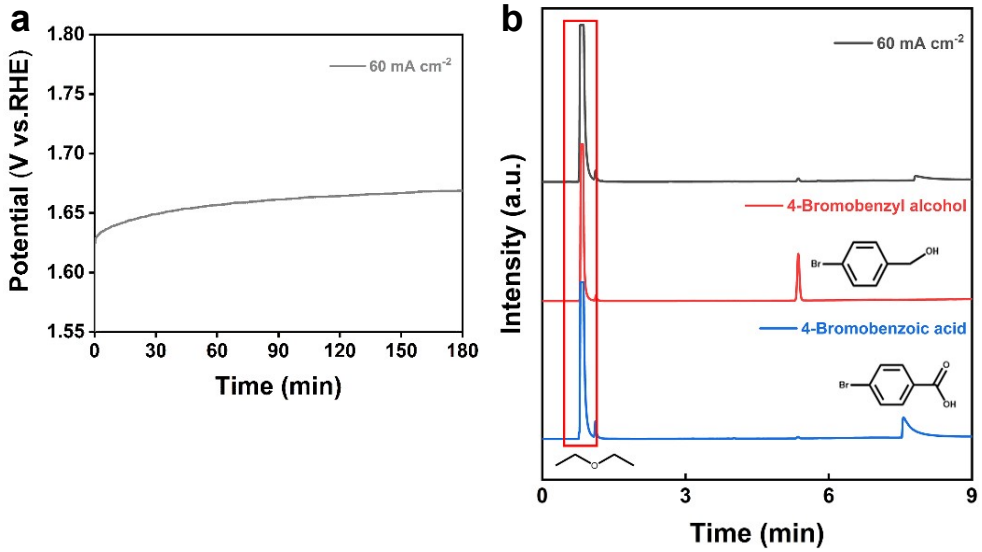

Fig.S19 (a) The chronopotentiometry curve of $NiCo_2O_4$/NF at the current density of 60 mA cm^{-2} in 1.0 M KOH solution containing 10 mM 4-bromobenzyl alcohol. (b) GC chromatograms of 4-bromobenzyl alcohol, 4-bromobenzoic acid and the electrolyte after 3 h anodic 4-bromobenzyl alcohol oxidation.

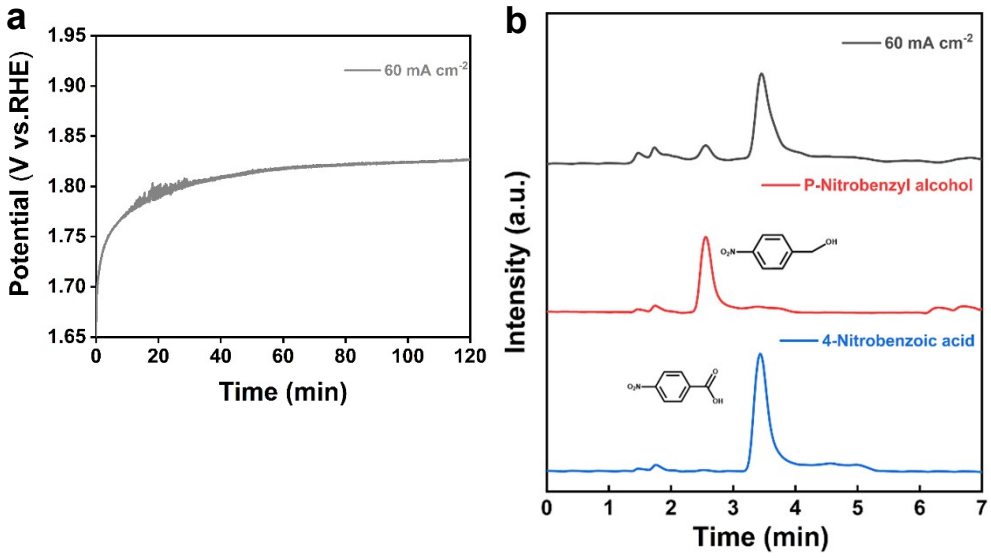

Fig.S20 (a) The chronopotentiometry curve of $NiCo_2O_4$/NF at the current density of 60 mA cm^{-2} in 1.0 M KOH solution containing 10 mM p-nitrobenzyl alcohol. (b) HPLC chromatograms of p-nitrobenzyl alcohol, 4-nitrobenzoic acid, and the electrolyte after 2 h anodic p-nitrobenzyl alcohol oxidation.

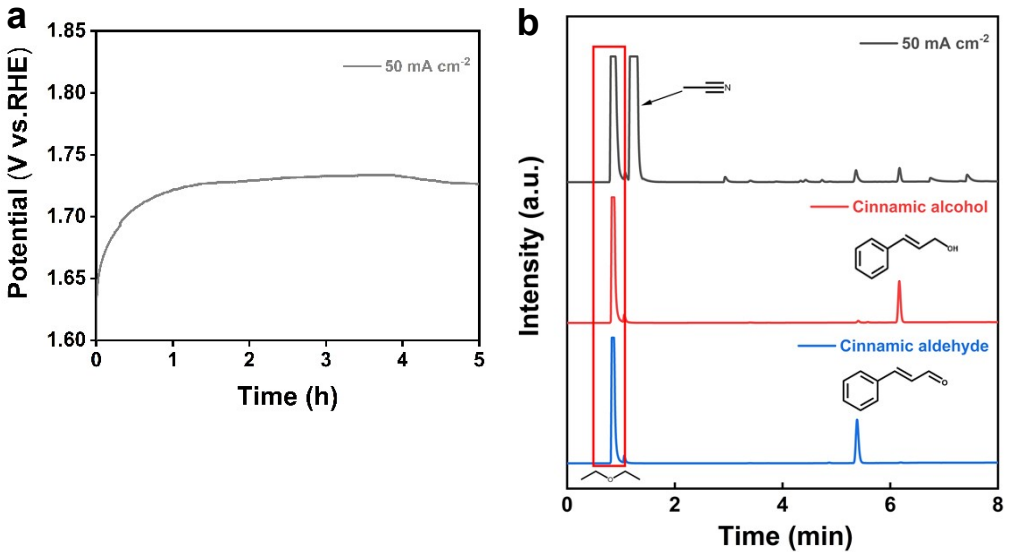

Fig.S21 (a) The chronopotentiometry curve of $NiCo_2O_4$/NF at the current density of 50 mA cm^{-2} in 1.0 M KOH solution containing 10 mM cinnamic alcohol. (b) GC chromatograms of cinnamic alcohol, cinnamic aldehyde and the electrolyte after 5 h anodic cinnamic alcohol oxidation.

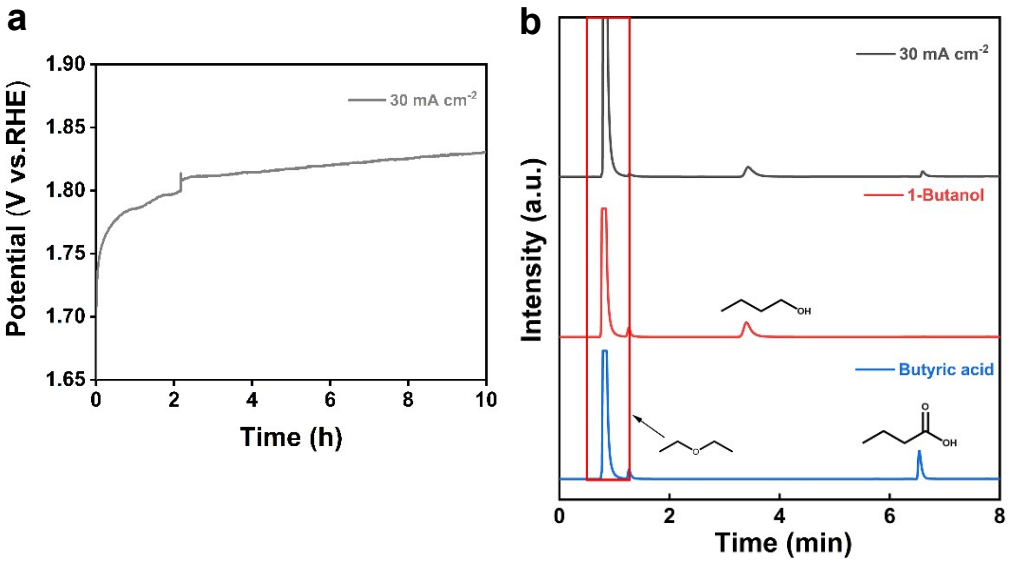

Fig.S22 (a) The chronopotentiometry curve of $NiCo_2O_4$/NF at the current density of 30 mA cm^{-2} in 1.0 M KOH solution containing 20 mM 1-butanol. (b) GC chromatograms of 1-butanol, butyric acid and the electrolyte after 10 h anodic 1-butanol oxidation.

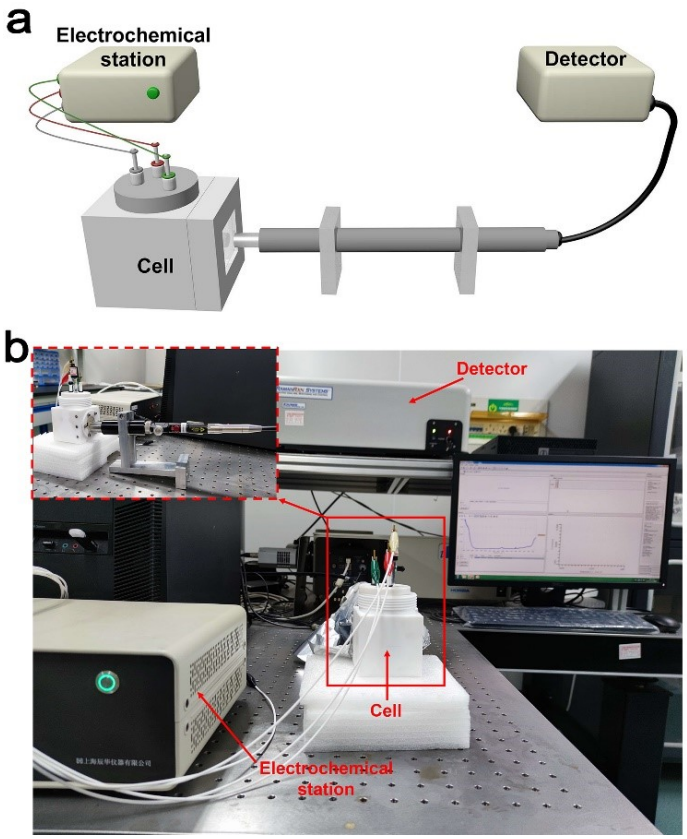

Fig.S23 (a) The schematic diagram and (b) photograph of the in situ Raman testing process.

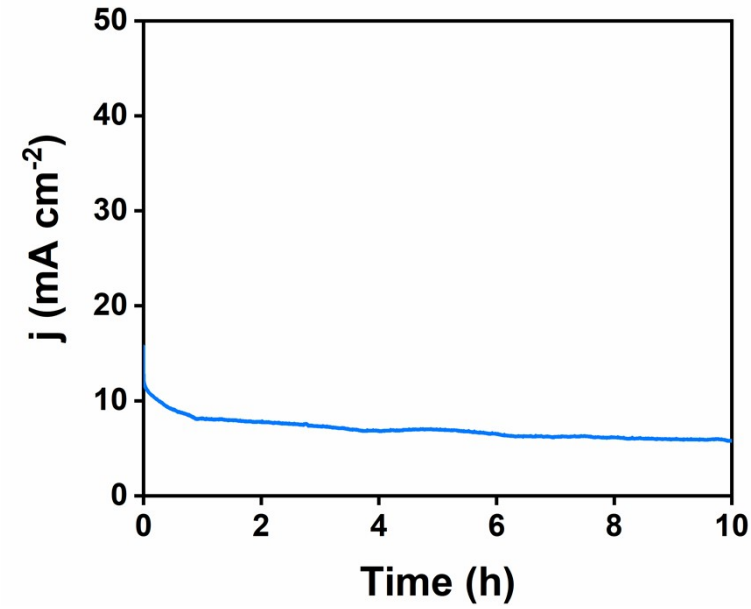

Fig. S24 Water-splitting durability tests for $NiCo_2O_4$/NF in 1.0 M KOH.

Table S1. Comparison of $NiCo_2O_4$/NF and other electrocatalysts on electrooxidation of benzyl alcohol to benzoic acid.

Catalyst	Electrolyte	Main product	Time (min)	Conv (%)	Sel (%)	FE (%)	Reference
$NiCo_2O_4$/NF	50mM BA + 1 M KOH	Benzoic acid	120	96.4	99	60.4	This work
Ni foam	50mM BA + 1 M KOH	Benzoic acid	120	76.8	73.3	55.3	This work
Co_3O_4 NWs/Ti	10mM BA + 1 M KOH	Benzoic acid		99	92	56.82	*ACS Nano*, 2017, **11**, 12365-12377
$Co_{0.83}Ni_{0.17}$/AC	10mM BA + 1 M KOH	Benzoic acid		100	99.4	96	*New J. Chem.*, 2018, **42**, 6381–6388.
1.0 h-$Ni(OH)_2$	40mM BA + 1 M KOH	Benzoic acid	140	99.99	99.3	98.62	*Green Chem.*, 2019, **21**, 578–588.

Table S2. Electrooxidation of different substrates by using $NiCo_2O_4$/NF.

Entry	Substrate	Product	Concentration (mM)	j (mA cm^{-2})	Potential (V vs. RHE)	Time (h)	Conv. (%)	Yield (%)	Sel. (%)
1			50	30	—	3	70.4	6	8.5
2	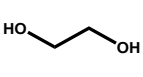		40	—	1.6	2	66.5	16.0	24.1
3	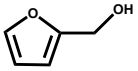	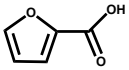	10	—	1.75	2	99.9	50.2	50.2
4	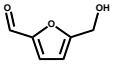	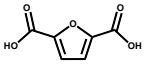	10	20	—	2.25	98.2	75.9	77.3
5		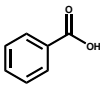	50	—	1.6	2	93.6	92.8	99.2
6	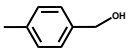	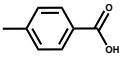	10	40	—	5	69.3	65.5	94.5
7	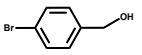	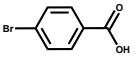	10	60	—	3	93.1	93.1	100
8	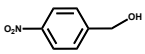	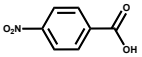	10	60	—	2	91.6	90.7	99.0
9	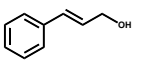	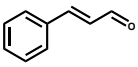	10	50	—	5	82.4	16.2	19.7
10	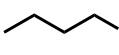	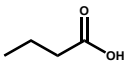	20	30	—	10	24.1	24.1	100

Reaction conditions: $NiCo_2O_4$/NF (1 cm^{-2}), 1.0 M KOH. The products were determined by ^{1}H NMR, GC and HPLC analysis.